Journal of Alloys and Compounds 509 (2011) 4583–4587

Contents lists available at ScienceDirect

Journal of Alloys and Compounds

journal homepage: www.elsevier.com/locate/jallcom

Phase selection during calcium silicide formation for layered and powder growth

Cuilian Wen[a], Akihiko Kato[b], Tomomi Nonomura[c], Hirokazu Tatsuoka[a,c,*]

[a] Graduate School of Science and Technology, Shizuoka University, 3-5-1 Johoku, Naka-ku, Hamamatsu, Shizuoka 432-8011, Japan
[b] FDK Corporation, 2281 Washizu, Kosai 431-0495, Japan
[c] Faculty of Engineering, Shizuoka University, 3-5-1 Johoku, Naka-ku, Hamamatsu, Shizuoka, 432-8561, Japan

ARTICLE INFO

Article history:
Received 13 November 2010
Received in revised form 17 January 2011
Accepted 18 January 2011
Available online 22 January 2011

Keywords:
Interfaces
Growth from vapor
Calcium compounds
Semiconducting silicon compounds

ABSTRACT

Phase selection during Ca silicide formation was discussed using the chemical potential and the effective heat of formation ($\Delta H'$) models. The compositional analyses of Ca silicides were experimentally carried out in detail for both the layered and powder growth process. Based on the calculation, the Ca_2Si phase has the largest negative $\Delta H'$ and is the first phase to form in the Ca–Si system. In addition, the total energy consideration consisting of the formation energy of each phase and interfacial energy between two adjoining phases is proposed to explain the experimental results of phase selection in the Ca silicide formation.

1. Introduction

Recently, semiconducting silicides have attracted much attention as environmentally conscious materials, which consist of non-toxic and abundant materials. The solid phase interaction between thin metal films and silicon has been widely studied because of the importance of silicides as interconnects and contacts in silicon devices.

The phase formation and transformation of multi-component compound systems have been intensively discussed based on thermodynamic considerations [1–8]. For the case of phase formation and phase stability, thermodynamic descriptions were developed using thermodynamic models for Cr–Sn–Ti [1] and Al–Zn–Mg–Si [2]. The chemical potentials consideration was made for the growth of gold-seeded III–V semiconductor nanowires [3]. On the other hand, for the case of growth phase evolution, the preferable phase formation or phase selection was investigated under the consideration of thermodynamics for Mg–Sn–Si and Mg–Sn–Si–Ca [4] and Fe–Co [5]. The phase transformation or the solidification pathways was investigated for from anantase to rutile [6], Mg–Pd nanoparticles [7] and Mg–Zn–Y–Zr alloys [8].

For considering the silicide growth, there has been considerable interest in formulating rules for predicting the first silicide phase which forms as well as the sequence of subsequent phases [9–11]. These rules heavily rely on phase diagram information such as the lowest eutectic, stability and diffusion species, but do not directly use thermodynamic data. Some metal–silicons, such as the Cr–Si, Co–Si and Ni–Si systems have been extensively discussed [11–13]. However, there are few reports on the phase selection during the silicide formation of the Ca–Si system. Ca silicide powders and films have been grown on Si or Si/Mg_2Si powders or substrates by heat diffusion treatments [14–18], however, it is still difficult to grow high quality single phase Ca silicide. There are multiple silicide phases, such as $CaSi_2$, CaSi, Ca_5Si_3 and Ca_2Si that exist in the Ca–Si system, which could lead to the simultaneous formation during its growth [14–17]. Among them, Ca_2Si and Ca_5Si_3 have been reported to have a semiconducting behavior [14,15,19]. It is important to understand the elemental chemical potential gradients and effective heat of formation (EHF) as certain driving forces for diffusion in the Ca–Si system, in addition to the concentration controlled phase selection.

Experimentally, Ca-silicide formations were reported in Refs. [16,19], which reported for the layered growth, the Ca_2Si and CaSi interface was formed while the Ca_5Si_3 phase was not significantly formed. On the other hand, for powder growth, the Ca_5Si_3 single phase powders were grown. However, a detailed compositional analysis has not been carried out.

In this study, the compositional analysis of Ca-silicides was made for both the layered and powder growth processes. In addition, the phase selection during the Ca silicide formation was discussed based on the chemical potential and the effective heat of formation ($\Delta H'$) models associated with the additional interfacial energy to explain the experimental Ca silicide layered and powder growth processes.

* Corresponding author at: Faculty of Engineering, Shizuoka University, 3-5-1 Johoku, Naka-ku, Hamamatsu, Shizuoka 432-8561, Japan. Tel.: +81 53 478 1099; fax: +81 53 478 1099.
E-mail address: tehtats@ipc.shizuoka.ac.jp (H. Tatsuoka).

0925-8388/$ – see front matter © 2011 Elsevier B.V. All rights reserved.
doi:10.1016/j.jallcom.2011.01.112

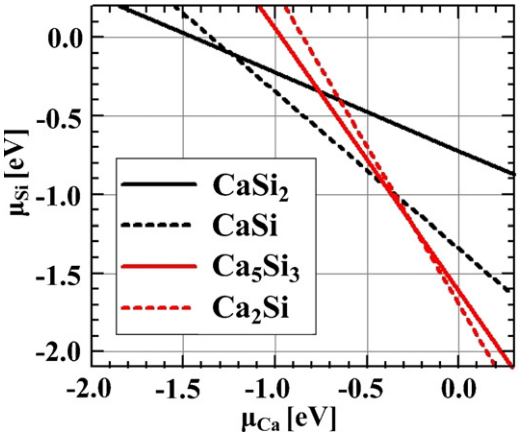

Fig. 1. The calculated two-dimensional chemical potential diagram of $CaSi_2$, CaSi, Ca_5Si_3 and Ca_2Si phases for the Ca–Si system. The origins of each chemical potential are set to the bulk ones, μ_{Ca}^{bulk} and μ_{Si}^{bulk}.

2. Experimental

As the first step in the silicide layer growth, Mg_2Si layers were grown on Si substrates prior to the Ca_2Si growth. The Mg source and Si substrates were placed in a loosely sealed quartz container, which was loaded into a vacuum chamber. The container was then heated and the temperature was maintained at 370 °C. The growth procedure of the Ca_2Si layer is basically the same as the Mg_2Si growth, except for the growth temperature and growth time. The Ca_2Si layers were grown by the heat treatment of Mg_2Si/Si (1 1 1) substrates at 600 °C in Ca vapor for 3 h [16].

The Ca_5Si_3 powders were synthesized by exposure of the Si powder to Ca fluxes. The Ca source and Si powder were first placed in a loosely sealed glass container, and then the container was loaded into a vacuum chamber. The container was then heated and the temperature was maintained at 750 °C for 12 h [19].

The structural properties of the resultant layers and powders were characterized by scanning electron microscopy (SEM) measurements. In addition, the compositional analysis was completed using energy dispersive X-ray spectroscopy (EDS).

The two-dimensional chemical potential diagram of the $CaSi_2$, CaSi, Ca_5Si_3 and Ca_2Si phases for the Ca–Si system was calculated by a first principles scheme based on the local density functional theory. It was postulated that the Ca_mSi_n phase is grown under thermodynamically equilibrium conditions which is characterized by the chemical potentials of the constituent elements, μ_{Ca} and μ_{Si}. The following expression should be satisfied:

$$\mu_{Ca_mSi_n} \leq m\mu_{Ca} + n\mu_{Si} \quad (1)$$

where $\mu_{Ca_mSi_n}$ is the chemical potential of Ca_mSi_n per one chemical formula. Furthermore, if no segregation in Ca_mSi_n occurred, the following conditions should be added:

$$\begin{aligned} &\mu_{Ca_mSi_n} = m\mu_{Ca}^{bulk} + n\mu_{Si}^{bulk} - \Delta G_{Ca_mSi_n}, \quad \Delta G_{Ca_mSi_n} > 0, \\ &\mu_{Ca} < \mu_{Ca}^{bulk}, \qquad\qquad \mu_{Si} < \mu_{Si}^{bulk}, \end{aligned} \quad (2)$$

where μ_{Ca}^{bulk} and μ_{Si}^{bulk} are the chemical potentials of bulk Ca and Si crystals, respectively, and $\Delta G_{Ca_mSi_n}$ is the heat of formation. The $\mu_{Ca_mSi_n}$, μ_{Ca}^{bulk} and μ_{Si}^{bulk} values were obtained by first principles total energy calculations (the entropy contributions was neglected). Our total energy calculation scheme is described in Ref. [20].

3. Results and discussion

The two-dimensional chemical potential diagram for Ca silicide phases is shown in Fig. 1. The stable domain of each stoichiometric phase is defined by a line, because the sum of the chemical potentials of the different components weighted by the appropriate stoichiometric coefficient is equal to the Gibbs energy of formation of the phase. The points of intersection of the two lines identify the two-phase equilibriums. The planes, defined by the intersection of the corresponding lines, represent the corresponding phase's coexisting field. It is noted that the stable domain of the single-phase only existed in the line of no planes with the other lines, called the single-phase line. It was found that all of the binary phases mentioned here have a certain stable domain as shown by the single-phase lines in the figure. In addition, it is noted that the $CaSi_2$, CaSi, and Ca_2Si have relatively larger stable single-phase domains compared to the Ca_5Si_3 phase, which suggests that the Ca_5Si_3 single-phase formation window is narrower than that of the other phases.

The heats of formation (ΔH^o) of the Ca silicide phase is calculated from the potential energies shown in Fig. 1 according the formula shown below:

$$\mu_{Ca_mSi_n} = m\mu_{Ca} + n\mu_{Si} - \Delta G_{Ca_mSi_n} \quad (3)$$

Assuming the equilibrium condition, $\Delta G_{Ca_mSi_n} = 0$, $\mu_{Ca_mSi_n}$ is the chemical potential for $m \times \mu_{Ca} + n \times \mu_{Si}$ in the Ca_mSi_n phases. From Fig. 1, it is calculated as −1.44, −1.34, −4.84 and −1.70 eV for $CaSi_2$, CaSi, Ca_5Si_3 and Ca_2Si, respectively. The heat of formation energy for 1 mol is obtained as:

$$\Delta H^o = N_A \times \mu_{Ca_mSi} \quad (4)$$

where N_A is the Avogadro constant of 6.02×10^{23} mol^{-1}. The calculated heat of formation energy for each phase is listed in Table 1. In addition, most available phase equilibriums and thermodynamic data for the Ca–Si system have been collected and critically evaluated by Heyrman et al. [21]. Some ΔH^o calculated from the literature [22–24] is also shown in the table, which is in excellent agreement with our calculated results.

The driving force for a process to take place is given by the change in the Gibbs free energy:

$$\Delta G = \Delta H - T\Delta S \quad (5)$$

where ΔH is the change in enthalpy (or heat of formation) during the reaction at temperature T and ΔS is the change in entropy. For the solid state interactions, $\Delta S \approx 0$ and ΔG is thus approximated by the change in ΔH during the reaction. However, the first formed phase is not only determined by the lowest heat of formation, but also by the concentration of atoms at the growth interface available to participate in the reaction. The effective concentration differs from the physical concentration at the growth interface and cannot be directly calculated [12,25–27]. The effective heat of formation ($\Delta H'$) of the Ca silicide phases is calculated as a function of the concentration, and is given by the Ca–Si phase diagram in Fig. 2. A general definition of the $\Delta H'$ is given in Ref. [11]. It is clear that all the phases have a negative $\Delta H'$ and thus the release of the energy from the system occurs when the concentrations of Ca and Si match that of the composition of a particular compound. In order to determine the phase that will be formed, it is necessary to know the effective concentration of the elements at the growth interface. Generally, the intermixing at the interface during the solid phase reaction is expected to take place at the concentration of the lowest temperature eutectic of the binary system. In the case of the Ca-Si system, this occurs at a composition of 3.5 at% Si as shown in Fig. 2.

A rule for the first phase formation can thus be formulated which state the following: the first silicide compound to form during the metal–silicon interaction is the congruent phase with the most negative $\Delta H'$ at the concentration of the lowest temperature eutectic of the binary system [11]. The value of $\Delta H'$ has been calculated for the Ca–Si system at the lowest melting eutectic composition in Table 1. It is shown that CaSi has the largest negative ΔH^o of −15.6 kcal/g atom. However, at the lowest temperature eutectic point (3.5 at% Si), the limiting element is Si, and the Ca_2Si phase has the largest negative $\Delta H'$ of −1.4 kcal/g atom. Thus, it is expected that Ca_2Si is to be the first phase to form in the Ca–Si system.

During the normal Ca silicide formation, the effective concentration at the growth interface is controlled by the lowest eutectic. At this concentration, according to the EHF model, it can be seen that Ca_2Si has the largest negative $\Delta H'$ and is expected to form first as shown in Fig. 2. For thin Ca on thick silicon, all the Ca will be consumed to form Ca_2Si, and the effective concentration moves to the right side of the EHF diagram. According to the theory, Ca_5Si_3

Table 1
Heats of formation (ΔH^{o}) and the effective heat of formation ($\Delta H'$) calculated for the lowest-melting eutectic composition for the Ca–Si system.

Phase	Composition	ΔH°		Limiting element	$\Delta H'$ (kcal/g at.)	ΔH° [14] (kcal/g at.)	ΔH° [15] (kcal/g at.)	ΔH° [16] (kcal/g at.)
		(kcal/g mol)	(kcal/g at.)					
Lowest eutectic = $Ca_{0.965}Si_{0.035}$								
$CaSi_2$	$Ca_{0.333}Si_{0.667}$	−33.4	−11.1	Si	−0.6	−12.0	−9.0	−12.0
CaSi	$Ca_{0.500}Si_{0.500}$	−31.1	−15.6	Si	−1.1	−18.0	−11.9	−14.4
Ca_5Si_3	$Ca_{0.625}Si_{0.375}$	−111.8	−14.0	Si	−1.3	–	−13.2	–
Ca_2Si	$Ca_{0.667}Si_{0.333}$	−39.2	−13.1	Si	−1.4	−16.7	−13.4	−16.7

formation should lead to the largest negative $\Delta H'$ until the effective concentration is about 65 at% Ca is reached. After complete transformation of Ca_2Si to Ca_5Si_3, the effective Ca concentration at the growth interface further decreases to a concentration of less than about 55 at% Ca, thus the CaSi formation is thermodynamically favored. While after reaching 35 at% Ca, $CaSi_2$ formation is favored.

To examine the phase selection during the Ca silicide formation for the layered growth experimentally, selection of the substrate material is important to obtain the Ca-silicide layered structure. For the growth of Ca-silicide layers directly on Si substrates, the resultant Ca-silicides were easily removed from the Si substrates by an external stress, because of the formation of $CaSi_2$ phase with trigonal–rhombohedral stacking sequence structure, as reported previously [16]. On the other hand, Ca_2Si layers were successfully grown on Mg_2Si/Si substrates [16]. Thus, the Mg_2Si/Si substrates were employed for the Ca-silicide layered growth.

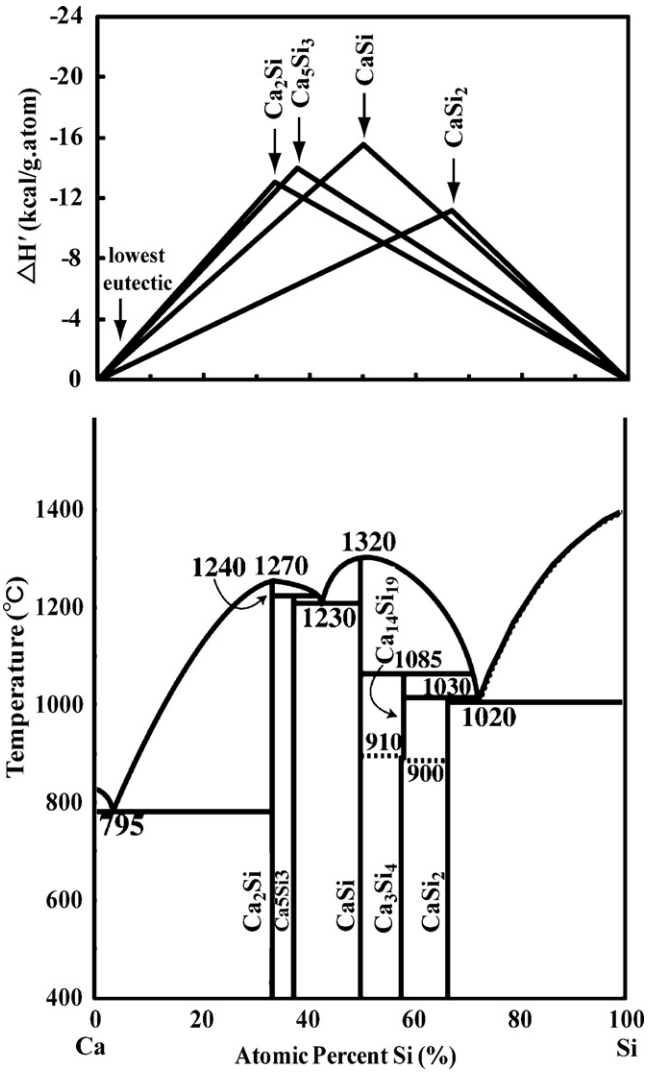

Fig. 2. The effective heat of formation ($\Delta H'$) and phase diagram [28] for the Ca–Si system. Each triangle in the effective heat of formation diagram represents the energy released as a function of the concentration during the formation of a particular calcium silicide phase.

Fig. 3 shows the cross-sectional SEM micrograph and the corresponding EDS analysis for the Ca_2Si/CaSi interface made by the Ca-silicide layered growth. It is found that no evidence of the formation of the Ca_5Si_3 phase is observed between the Ca_2Si and CaSi layers.

As shown in Figs. 1 and 2, Ca_5S_3 is one of stable phases, though the Ca_5Si_3 single-phase formation window is narrower than that of the other phases. However, the un-formation of the Ca_5Si_3 phase cannot be explained by the formation energy of each material.

In fact, it is possible to grow the Ca_5Si_3 phase as shown in Fig. 4, which shows the SEM micrograph and the corresponding EDS analysis for the particles of the resulting powders. The powders are confirmed to be Ca_5Si_3 by the XRD spectrum in Ref. [19]. The morphology and the EDS analysis showed powder size of about ~200 μm and the compositionally homogeneous compound is formed through the powders.

Even though the Ca_5Si_3 phase has a narrower growth window as shown in Figs. 1 and 2, if the appropriate Ca and Si concentration ratio and the growth condition could be preferably chosen, the Ca_5Si_3 single-phase compound can be successfully obtained, as expected for the second nucleation phase in the EHF consideration. For the powder growth, when the powder size is smaller, the boundary condition is not fixed, and the composition of any part of the powder can be maintained at the same composition, and the composition of the powder is determined by the growth conditions.

On the other hand, not only Ca_2Si, but also the CaSi phase was grown, and formation of the Ca_5Si_3 phase was skipped during the experiment. The EHF consideration does not explain this phenomenon, but might be explained as follows. For the layered growth, the boundary conditions are always fixed, for example, the Ca-silicide phases are formed between the Si substrate and the deposited Ca. This growth condition causes the formation of a layered structure with a distinct compositional gradient from the substrate to the layer surface. The domains or substrates with 100% Si always exist on one side of the reaction region. It is considered that the Si rich silicide phases are formed when the Ca flux through the silicide layers to Si layers (substrate) decreases. It would also be possible that the second lowest eutectic affects the silicide formation in the Si-rich region.

As already mentioned, the formation energy consideration cannot explain the formation of the Ca_2Si/CaSi structure. The total energy consideration consisting of the formation energy of each phase and interfacial energy between two adjoining phases is proposed to explain the formation of the structure. As shown in Fig. 3, the Ca_2Si/CaSi interface is formed, while no formation of the Ca_5Si_3 phase is observed for the layered growth. The structure is schematically illustrated in Fig. 5(a).

Assuming that a part of the Ca_2Si/CaSi interface region is transformed into the Ca_5Si_3 phase, a Ca_5Si_3 layer with a thickness of c = 1.46 nm (the largest lattice constant) between the Ca_2Si and CaSi

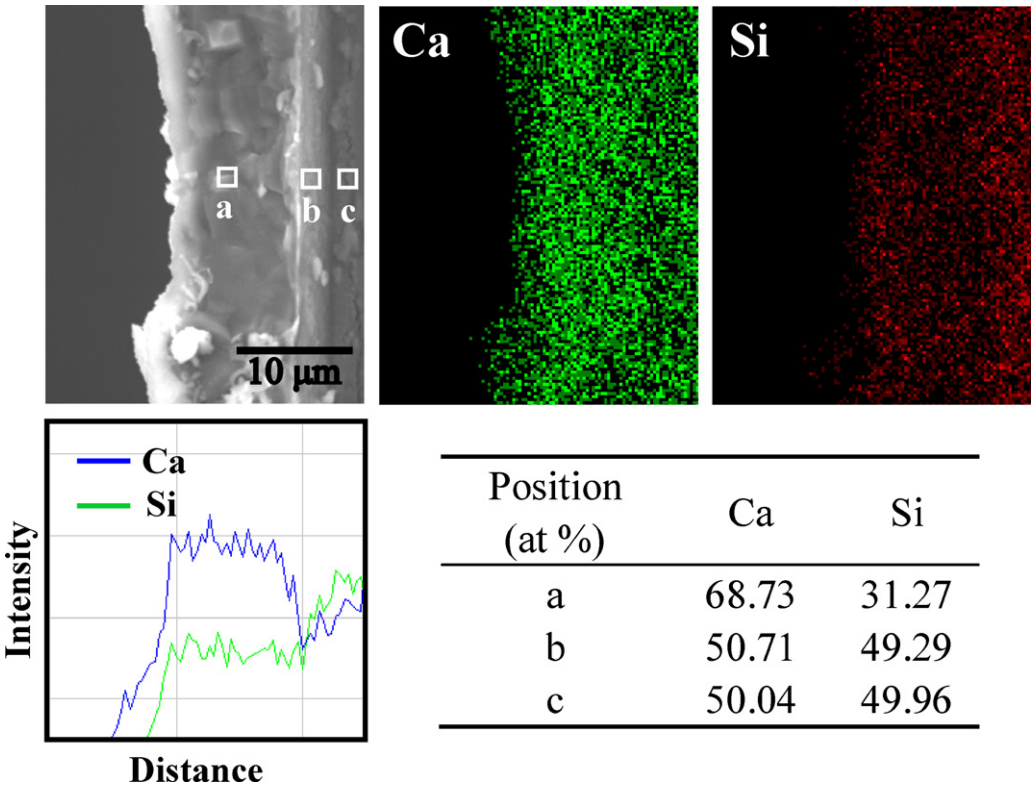

Position (at %)	Ca	Si
a	68.73	31.27
b	50.71	49.29
c	50.04	49.96

Fig. 3. The cross-sectional SEM micrograph and the corresponding EDS analysis for the resulting layers grown at 600 °C for 3 h.

regions is formed, as shown in Fig. 5(b). The phase transformation reaction is shown as:

$$2Ca_2Si + CaSi \rightarrow Ca_5Si_3. \quad (6)$$

The number of Ca and Si atoms should be equal for both cases shown in Fig. 5(a) and (b). Thus, the amounts of the substances in each region should be n_{A2} (mol) = $2 \times n_{B1}$(mol) and n_{C2} (mol) = n_{B1}(mol). Assuming the interface area of the layers is a unit area, namely, 1 cm^2, the calculated amounts of the substances are shown in the Fig. 5 table. The A1 and C1 layers are not listed, because the internal energy is not changed for the cases whether or not Ca_5Si_3 is formed.

The sum of the internal energy deduced from the heat of formation energy in each region, A2, C2 and B1, are -8.95×10^{-8}, -3.55×10^{-8} and -1.28×10^{-7} kcal, respectively. Comparing the internal energy for (a) $E_{A2+C2} = -1.25 \times 10^{-7}$ kcal with that for (b) $E_{B1} = -1.28 \times 10^{-7}$ kcal, the case (b) $Ca_2Si/Ca_5Si_3/CaSi$ structure is more thermodynamically favored than the case (a) $Ca_2Si/CaSi$

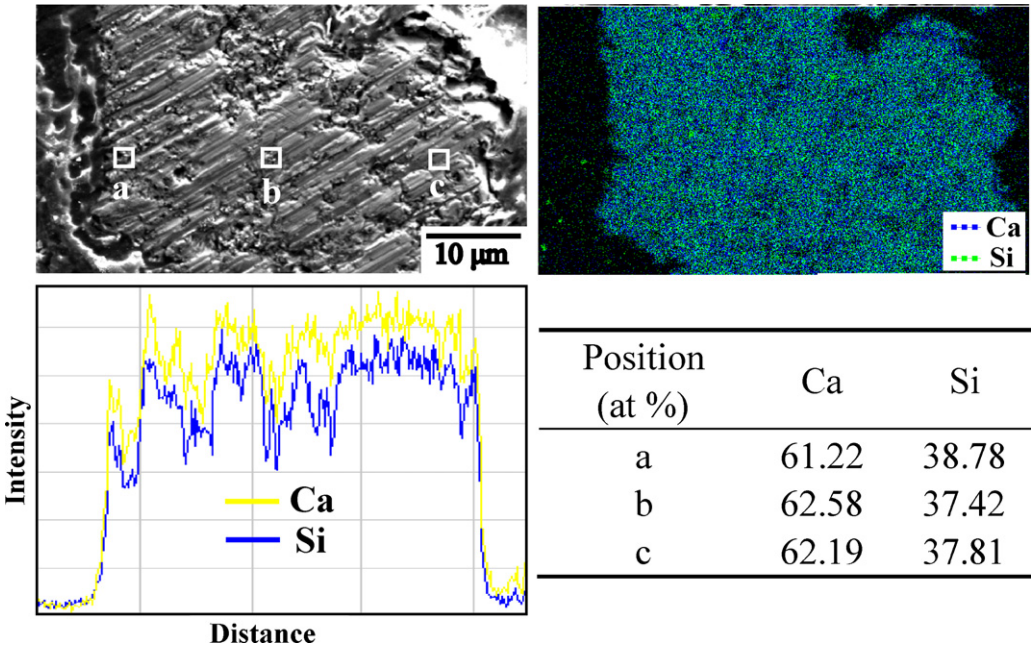

Position (at %)	Ca	Si
a	61.22	38.78
b	62.58	37.42
c	62.19	37.81

Fig. 4. SEM micrograph and the corresponding EDS analysis for the particles of the resulting powders grown at 750 °C for 12 h.

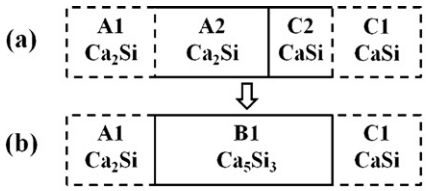

Position	Phase	Length (nm)	n (mol)	Energy (kcal)
B1	Ca_5Si_3	1.46	1.14×10^{-9}	-1.28×10^{-7}
A2	Ca_2Si	1.14	2.28×10^{-9}	-8.95×10^{-8}
C2	CaSi	0.33	1.14×10^{-9}	-3.55×10^{-8}

Fig. 5. Silicide formation model of $Ca_2Si/Ca_5Si_3/CaSi$ and $Ca_2Si/CaSi$ layer structures, and the corresponding calculated internal energy of the each phase.

structure, which is not consistent with the previously reported experimental results.

However, it should be pointed out that another new interface is formed when Ca_5Si_3 exists, namely, there is one interface for (a) $Ca_2Si/CaSi$, and there are two interfaces for the (b) $Ca_2Si/Ca_5Si_3/CaSi$ structures. Actually, it is difficult to calculate the interface energy for the Ca silicides. However, it is worthwhile to refer the typical values of interfacial energy for the reported silicide materials. It has been reported that the $TiSi_2$ interfaces energies are 900 ergs/cm^2 on silicon (1 0 0) and 600 ergs/cm^2 on silicon (1 1 1), respectively. For $ZrSi_2$, the interfaces energy is 800 ergs/cm^2 on silicon (1 1 1) [29]. Assuming that the interface energy E_{surf} is typically 800 ergs/cm^2, namely 1.91×10^{-8} kcal/cm^2, the total energy including the sum of the heat of formation energy and the interfacial energy are for (a) $E_{A2+C2}+E_{surf}=-1.06\times10^{-7}$ kcal and for (b) $E_{B1}+2\times E_{surf}=-8.93\times10^{-8}$ kcal. The result suggests that the formation of the interface increases the total energy of the structure. In this calculation, the actual values of the Ca silicide interfaces are not clear, however, it is certain that the additional interface formation increases the total energy of the structure, thus a multilayer structure does not tend to be realized. Thus, it could be concluded that the Ca_5Si_3 would not form between the Ca_2Si and CaSi layers when considering the narrower growth window of the Ca_5Si_3 as shown in Fig. 1.

4. Conclusions

Phase selection during calcium silicide formation was discussed using the chemical potential and the effective heat of formation ($\Delta H'$) models. The phase selection theory and Ca silicide interface model are discussed and compared to the experimental results. Experimentally, for the layered structure, no Ca_5Si_3 phase was formed between the Ca_2Si and CaSi phases. On the other hand, the single Ca_5Si_3 phase was formed during powder growth, and the stoichiometry distribution of the Ca_5Si_3 is homogeneous throughout the powders. In the calculation, the Ca_2Si phase has the largest negative $\Delta H'$ with the value of -1.4 kcal/g atom at the lowest temperature eutectic point (3.5 at% Si) and the first phase to form in the Ca–Si system. The proposed phase selection model including the potential energy and the additional interfacial energy successfully explains the experimental results, in which the Ca_5Si_3 phase would not form between the Ca_2Si and CaSi layers.

References

[1] Y.L. Gao, C.P. Guo, C.R. Li, Z.M. Du, J. Alloys Compd. 498 (2010) 130.
[2] Q. Li, Y.Z. Zhao, Q. Luo, S.L. Chen, J.Y. Zhang, K.C. Chou, J. Alloys Compd. 501 (2010) 282.
[3] F. Glas, J. Appl. Phys. 108 (2010) 073506.
[4] A. Kozlov, J. Gröbner, R. Schmid-Fetzer, J. Alloys Compd. 509 (2011) 3326.
[5] N. Liu, F. Liu, G.C. Yang, Y.Z. Chen, C.L. Yang, Y.H. Zhou, J. Alloys Compd. 467 (2009) L11.
[6] K. Prasad, D.V. Pinjari, A.B. Pandit, S.T. Mhaske, Ultrason. Sonochem. 17 (2010) 409.
[7] E. Callini, L. Pasquini, L.H. Rude, T.K. Nielsen, T.R. Jensen, E. Bonetti, J. Appl. Phys. 108 (2010) 073513.
[8] Z.H. Huang, S.M. Liang, R.S. Chen, E.H. Han, J. Alloys Compd. 468 (2009) 170.
[9] M. Ronay, Appl. Phys. Lett. 42 (1983) 577.
[10] R.Y. Zsaur, S.S. Lau, J.W. Mayer, M.-A. Nicolet, Appl. Phys. Lett. 38 (1981) 922.
[11] R. Pretorius, Vacuum 41 (1990) 1038.
[12] A. Vantomme, S. Degroote, J. Dekoster, G. Langouche, R. Pretorius, Appl. Phys. Lett. 74 (1999) 3137.
[13] J.W. Mayer, R. Pretorius, J. Appl. Phys. 81 (1997) 2448.
[14] Y. Warashina, Y. Ito, T. Nakamura, H. Tatsuoka, J. Snyder, M. Tanaka, T. Suemasu, Y. Anma, M. Shimomura, Y. Hayakawa, e-J. Surf. Sci. Nanotechnol. 7 (2009) 129.
[15] Y. Imamura, H. Muta, K. Kurosaki, S. Yamanaka, in: C. Uher, Y. Grin, Ballreich, Sugiwara, G. Pastorino, M. Cauchy, M. Udagawa (Eds.), 25th International Conference on Thermoelectrics, 2006, p. 535.
[16] H. Matsui, M. Kuramoto, T. Ono, H. Nose, H. Tatsuoka, H. Kuwabara, J. Cryst. Growth 237/239 (2002) 2121.
[17] T. Hosono, M. Kuramoto, Y. Matsuzawa, Y. Momose, Y. Maeda, T. Matsuyama, H. Tatsuoka, Y. Fukuda, S. Hashimoto, H. Kuwabara, Appl. Surf. Sci. 216 (2003) 620.
[18] N. Takagi, Y. Sato, T. Matsuyama, H. Tatsuoka, M. Tanaka, F. Chu, H. Kuwabara, Appl. Surf. Sci. 244 (2005) 330.
[19] T. Inaba, A. Kato, K. Miura, M. Akasaka, T. Iida, Y. Momose, H. Tatsuoka, Thin Solid Films 515 (2007) 8226.
[20] A. Kato, H. Rikukawa, Phys. Rev. B72 (2005) 041101(R).
[21] M. Heyrman, P. Chartrand, JPEDAV 27 (2006) 220.
[22] O. Kubaschewski, C.B. Alcock, International Series on Materials Science and Technology: Metallurgical Thermo-Chemistry, vol. 24, fifth ed., Pergamon Press, Oxford, 1979, p. 276.
[23] S. Brutti, A. Ciccioli, G. Balducci, G. Gigli, P. Manfrinetti, M. Napoletano, J. Alloys Compd. 317/318 (2001) 525.
[24] J.C. Anglezio, C. Servant, I. Ansara, CALPHAD 3 (1994) 273.
[25] R. Pretorius, A.M. Vredenberg, F.W. Saris, R. de Reus, J. Appl. Phys. 70 (1991) 3636.
[26] R. Pretorius, T.K. Marais, C.C. Theron, Mater. Sci. Eng. R 10 (1993) 1.
[27] R. Pretorius, Mater. Res. Soc. Symp. Proc. 25 (1984) 15.
[28] P. Manfrinetti, M.L. Fornasini, A. Palenzona, Intermetallics 8 (2000) 223.
[29] C.A. Sukow, R.J. Nemanich, J. Mater. Res. 9 (1994) 1214.